Supplementary Information for

Pressure-driven switching of magnetism in layered $CrCl_3$

Azkar Saeed Ahmad[1], Yongcheng Liang[2,*], Mingdong Dong[1], Xuefeng Zhou[1], Leiming Fang[3], Yuanhua Xia[3], Jianhong Dai[1,4], Xiaozhi Yan[1,4], Xiaohui Yu[4], Junfeng Dai[1], Guojun Zhang[2], Wenqing Zhang[1], Yusheng Zhao[1] & Shanmin Wang[1,*]

[1]Department of Physics and Shenzhen Engineering Research Center for Frontier Materials Synthesis at High Pressure, Southern University of Science and Technology, Shenzhen 518055, China. [2]College of Science, Institute of Functional Materials, and State Key Laboratory for Modification of Chemical Fibers and Polymer Materials, Donghua University, Shanghai 201620, China. [3]Key Laboratory for Neutron Physics, Institute of Nuclear Physics and Chemistry, China Academy of Engineering Physics, Mianyang 621999, China. [4]Key Laboratory of Extreme Conditions Physics, Institute of Physics, Chinese Academy of Sciences, Beijing 100190, China.

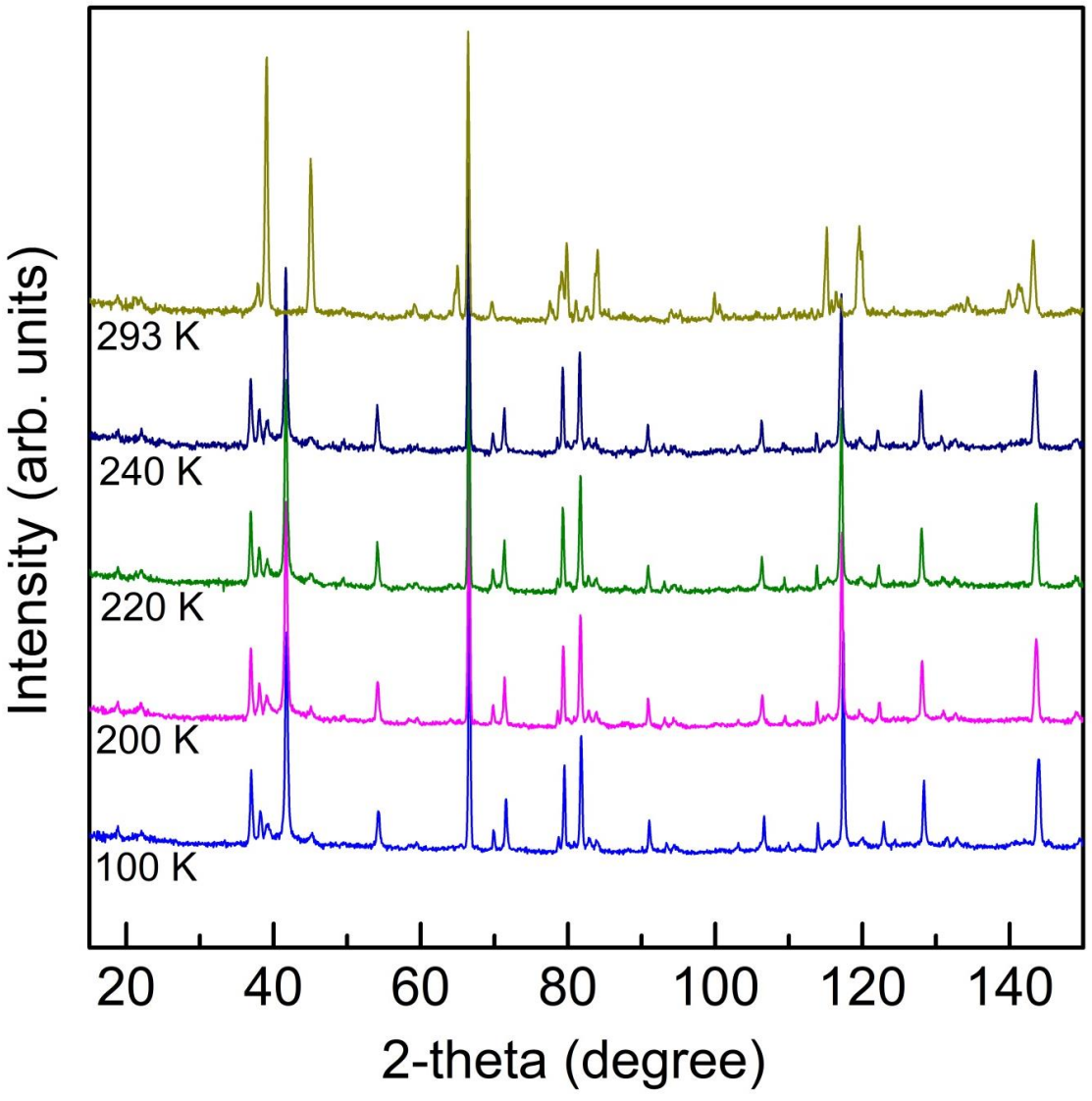

Fig. S1. Low-T neutron diffraction patterns for $CrCl_3$ collected during cooling from 293 K down to 100 K.

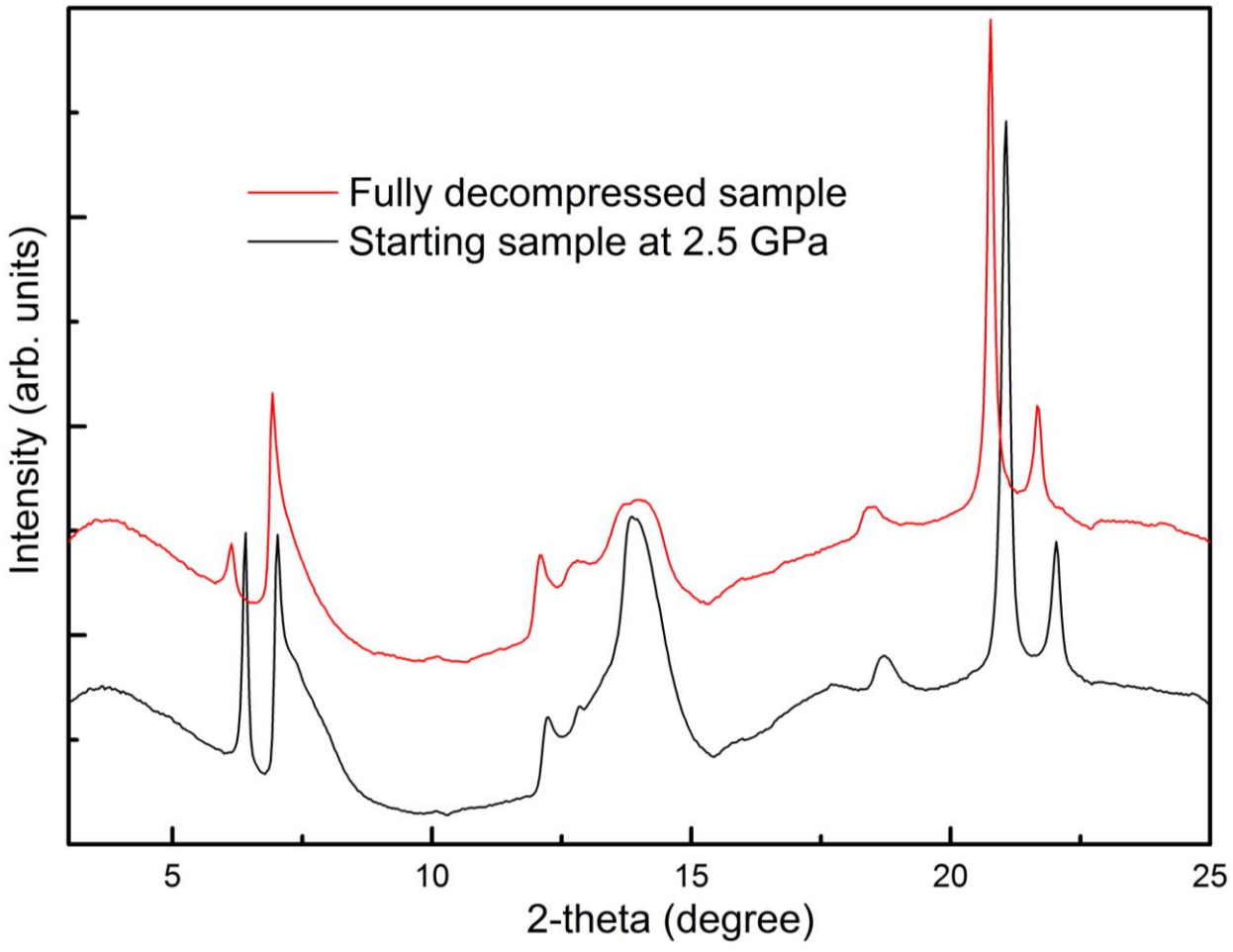

Fig. S2. XRD patterns of $CrCl_3$ at 2.5 GPa and the recovered material at ambient conditions.

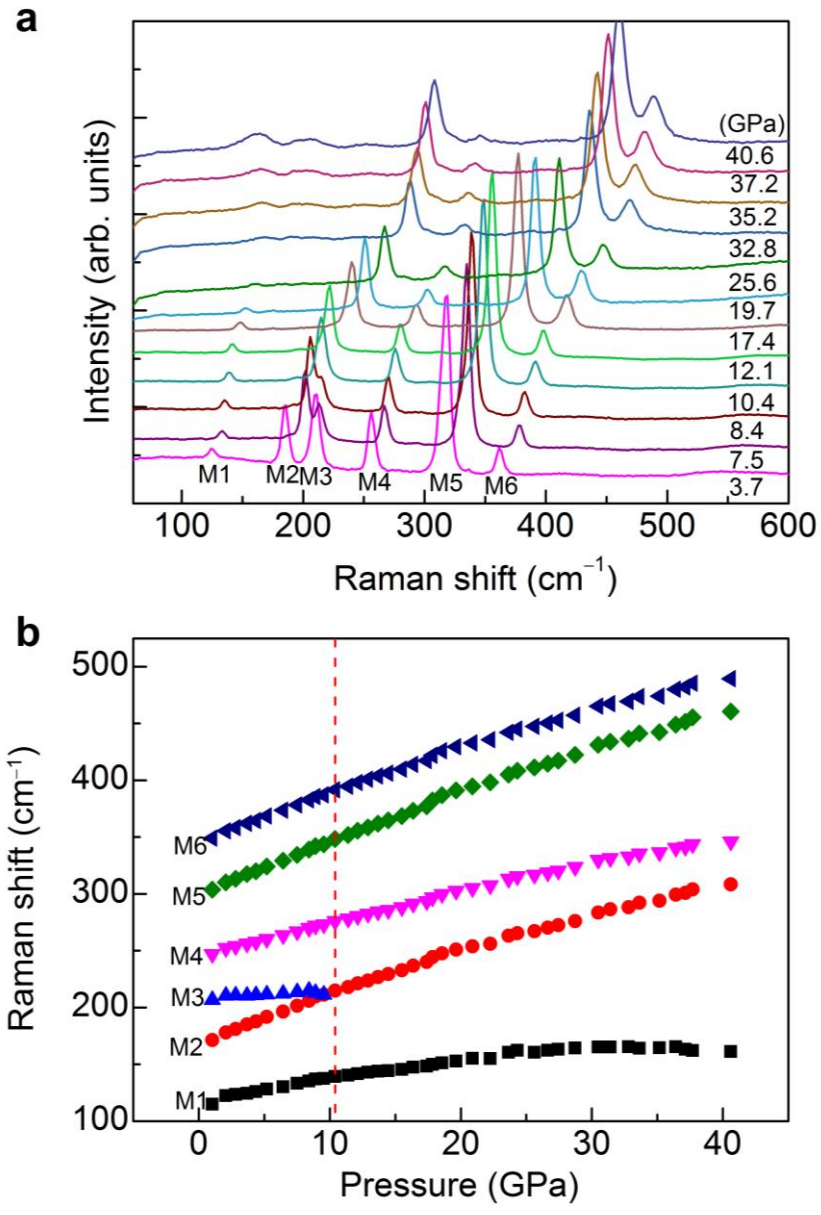

Fig. S3. The second experimental run of high-P Raman spectra of $CrCl_3$. (**a)** Raman spectra collected at selected pressures and room temperature. (**b)** Phonon frequency versus pressure. The vertical dashed red line serves as a visual guide.

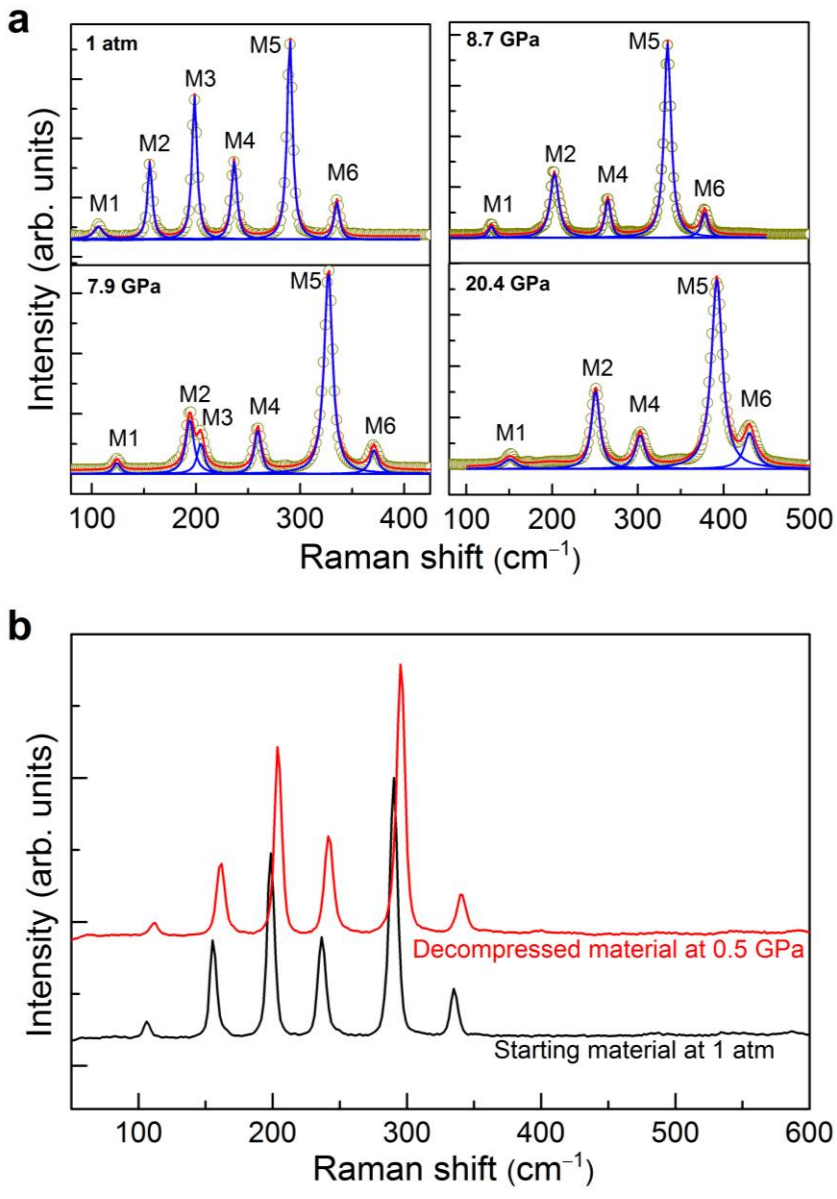

Fig. S4. High-P Raman spectra of $CrCl_3$ for the first experimental run. (**a)** Fitted Raman spectra for $CrCl_3$ at selected pressures. The open circles are the experimental data points and solid lines are the Lorentzian fits to the experimental data. (**b)** Comparison of Raman spectra of starting material and decompressed material.

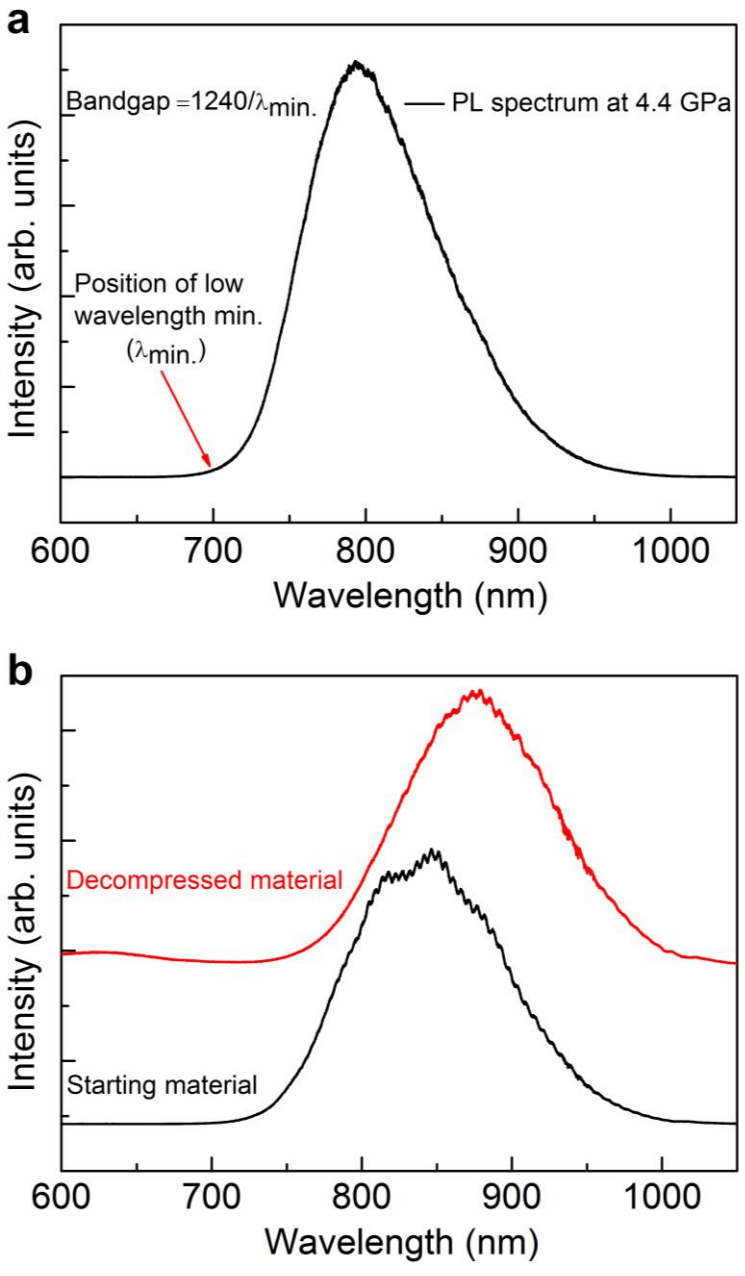

Fig. S5. The first experimental run of PL measurements for $CrCl_3$. **(a)** PL spectrum of $CrCl_3$ at 4.4 GPa. The spectrum edge on the low-wavelength side can be used for evaluation of bandgap. **(b)** PL spectra of starting material and decompressed material.

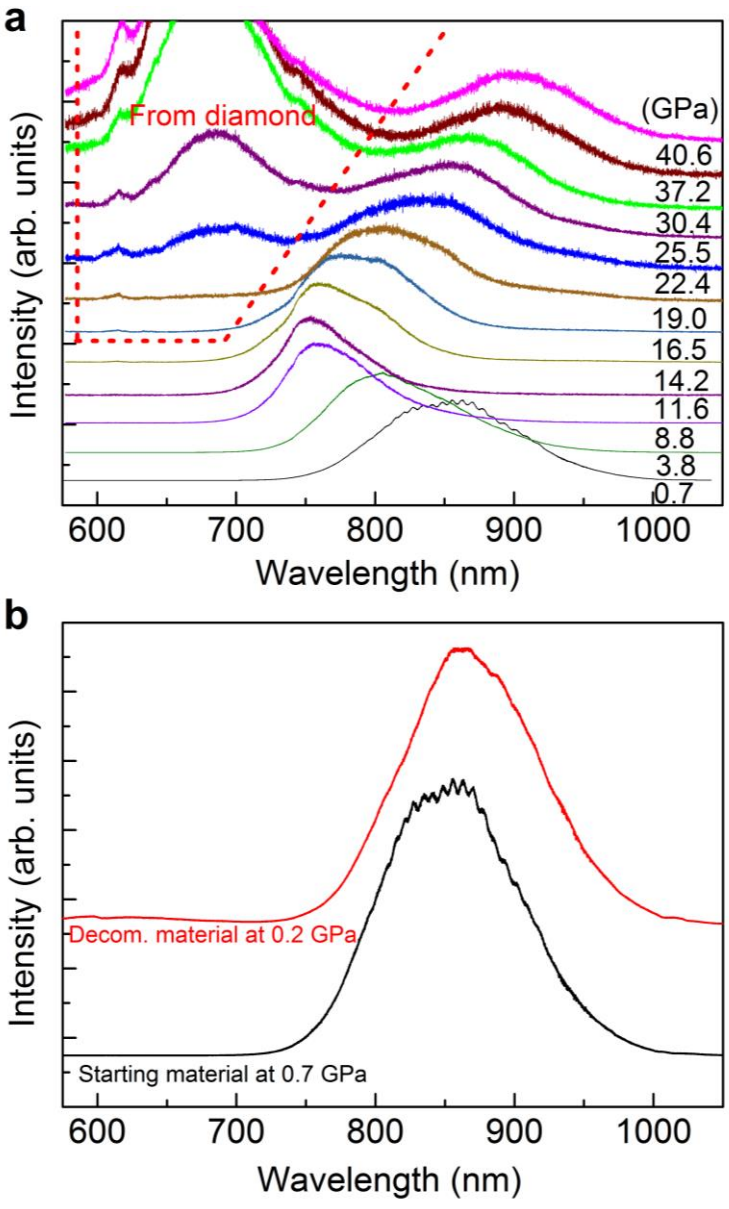

Fig. S6. The second experimental run for high-P PL measurements for $CrCl_3$. (**a)** Room-temperature PL collected at selected pressures. Above ~16.5 GPa, background signals from diamond become significant and are marked within the dashed lines. **(b)** PL spectra of starting material and decompressed material.

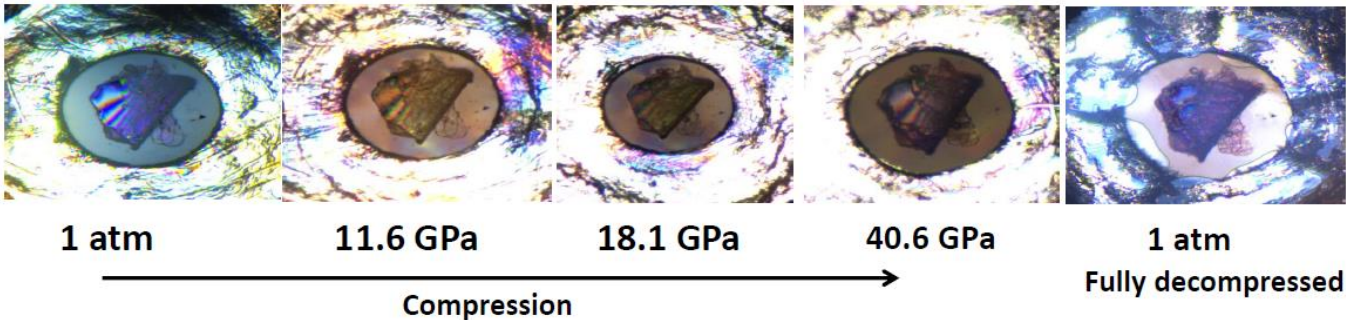

Fig. S7. High-P optical images of $CrCl_3$. Optical photographs (recorded with digital camera attached to Leica microscope) using a combination of reflected and transmitted light for illumination. The sample chamber is a hole of diameter ~120 μm drilled in a pre-indented T301 stainless steel gasket. The color changes correspond to the semiconductor-to-semiconductor transition under pressure. Upon decompression the original purple color of the specimen is retrieved, confirming the reversibility of semiconductor-to- semiconductor transition.

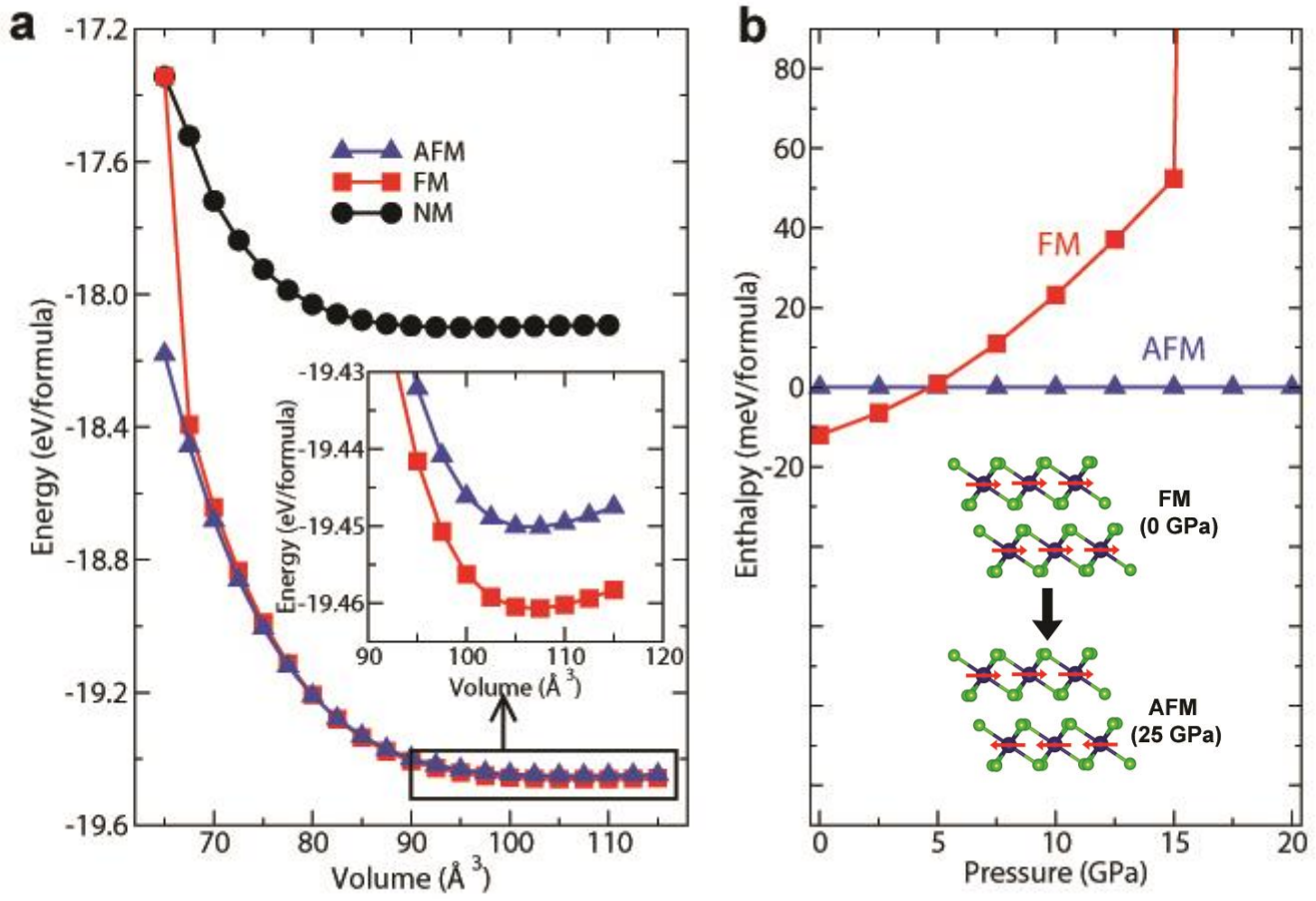

Fig. S8. Theoretical calculations of the total energy and enthalpy of $CrCl_3$ using the GGA method. (**a**) Calculated total energy versus volume of different magnetic phases (i.e., NM, FM, and AFM). (b) Calculated enthalpy versus pressure for the FM and AFM phases. The enthalpy of the AFM phase is set as the reference energy (i.e., set to zero) and all enthalpies are rescaled for one $CrCl_3$ formula. Insets are tentatively proposed magnetic structures for FM and AFM. The crossover from FM to AFM occurs under pressure.